Chemical Science

ROYAL SOCIETY OF CHEMISTRY

EDGE ARTICLE

View Article Online
View Journal | View Issue

Cite this: *Chem. Sci.*, 2023, **14**, 5912

All publication charges for this article have been paid for by the Royal Society of Chemistry

Pillar-layer Zn–triazolate–dicarboxylate frameworks with a customized pore structure for efficient ethylene purification from ethylene/ethane/acetylene ternary mixtures†

Jiaqi Liu,[a] Hao Wang *[a] and Jing Li *[ab]

Received 2nd March 2023
Accepted 3rd May 2023

DOI: 10.1039/d3sc01134h

rsc.li/chemical-science

The selective adsorption of C_2H_6 and C_2H_2 over C_2H_4 from $C_2H_2/C_2H_4/C_2H_6$ ternary mixtures for one-step C_2H_4 purification represents a crucial yet challenging task in industry. The pore structure of the adsorbents must be finely tailored to meet the demanding requirements for the separation considering the very similar physicochemical properties of the three gases. Herein, we report a Zn–triazolate–dicarboxylate framework, HIAM-210, featuring a novel topology which possesses one-dimensional channels decorated with adjacent uncoordinated carboxylate–O atoms. The suitable pore size and customized pore environment enable the compound to selectively capture C_2H_6 and C_2H_2 with high C_2H_2/C_2H_4 and C_2H_6/C_2H_4 selectivities of both 2.0. Breakthrough experiments show that polymer-grade C_2H_4 can be directly harvested from $C_2H_2/C_2H_4/C_2H_6$ (34/33/33 and 1/90/9) ternary mixtures. The underlying mechanism of the preferential adsorption was uncovered by grand canonical Monte Carlo simulations and DFT calculations.

Introduction

Ethylene (C_2H_4), the raw material for the production of various organic products, exceeded an annual global production of 200 million tons in 2022.[1–3] In the petrochemical industry, C_2H_4 is mainly produced through thermal cracking of naphtha or ethane where the crude products include ethane (C_2H_6) and acetylene (C_2H_2) as impurities.[4] The separation of C_2H_4 from C_2H_6 or C_2H_2 is currently a complex and energy-consuming process that involves solvent extraction or catalytic hydrogenation (C_2H_2 removal) and subsequent low-temperature distillation (C_2H_6 removal).[5,6] To this end, it is necessary and urgent to develop a simpler separation approach with lower energy consumption for C_2H_4 purification.[7,8]

Adsorptive separation based on physical adsorbents has emerged as an alternative means for industrial hydrocarbon separation.[9] However, the simultaneous removal of C_2H_2 and C_2H_6 from $C_2H_2/C_2H_4/C_2H_6$ mixtures remains a great challenge as the quadrupole moment and kinetic diameter of C_2H_4 (1.5×10^{-26} esu cm^2 and 4.1 Å) lie between those of C_2H_2 (7.2×10^{-26} esu cm^2 and 3.3 Å) and C_2H_6 (0.65×10^{-26} esu cm^2 and 4.4 Å) (Table S1†). Traditional adsorbents such as zeolites and activated carbons have not yet demonstrated the potential to meet the stringent requirements for the separation, mainly due to their limited structural tunability. In this context, metal–organic frameworks (MOFs), for which the pore size and chemical environment can be precisely adjusted, are considered promising candidates to address this challenging process.[10,11] In general, a non-polar surface favors C_2H_6 while smaller pore size prefers C_2H_2. However, since C_2H_2 has the lowest polarizability among the three hydrocarbons, a non-polar pore surface is also unfavorable for C_2H_2 adsorption, and most previously reported MOFs with high C_2H_6/C_2H_4 selectivity also possess low C_2H_2 uptake, insufficient for the efficient separation of $C_2H_2/C_2H_4/C_2H_6$ mixtures. Thus, the key to constructing MOFs for one-step C_2H_4 purification is to find the "sweet spot" by creating an optimal chemical environment on the pore surface and suitable pore size so as to achieve simultaneously high selectivities for both C_2H_2/C_2H_4 and C_2H_6/C_2H_4.

In this work, we present a new pillar-layer MOF constructed *via* zinc ions, triazole and a dicarboxylate linker (denoted as HIAM-210, HIAM = Hoffman Institution of Advanced Material), which combines suitable pore dimensions and a pore chemical environment for one-step separation of C_2H_4 from $C_2H_2/C_2H_4/C_2H_6$ ternary mixtures. The adjacent uncoordinated carboxylate–O atoms decorated on the pore surface act as strong binding sites for preferential adsorption toward C_2H_6 and C_2H_2 over C_2H_4, enabling HIAM-210 to have relatively high adsorption selectivities for C_2H_2/C_2H_4 (2.0) and C_2H_6/C_2H_4 (2.0), which exceed most of the MOFs previously tested for $C_2H_4/C_2H_6/C_2H_2$ separation, such as TJT-100 (1.8 and 1.2), ZJNU-115 (2.05 and

[a]*Hoffmann Institute of Advanced Materials, Shenzhen Polytechnic, 7098 Liuxian Blvd., Nanshan, Shenzhen 518055, Guangdong, P. R. China. E-mail: wanghao@szpt.edu.cn*
[b]*Department of Chemistry and Chemical Biology, Rutgers University, 123 Bevier Road, Piscataway, New Jersey 08854, USA. E-mail: jingli@rutgers.edu*

† Electronic supplementary information (ESI) available. CCDC 2244847. For ESI and crystallographic data in CIF or other electronic format see DOI: https://doi.org/10.1039/d3sc01134h

1.56), NUM-9 (1.50 and 1.62), NPU-2 (1.25 and 1.52), UPC-66 (1.05 and 1.65), *etc.*[12–16] Breakthrough experiments indicated that polymer-grade (99.95+%) C_2H_4 can be directly produced from ternary $C_2H_2/C_2H_4/C_2H_6$ mixtures. Grand canonical Monte Carlo (GCMC) simulations and DFT calculations provide important insights into the preferential adsorption mechanism at the molecular level.

Results and discussion

Yellow rod-shaped crystals of HIAM-210 were obtained by solvothermal reactions of $Zn(NO_3)_2 \cdot 6H_2O$, 1,2,4-triazole (TZ) and 1,4-naphthalene dicarboxylic acid (NDC) in *N*,*N*-dimethylformamide (DMF)/H_2O solution at 423 K (Fig. 1a and S1, see the ESI† for detailed synthesis). Single crystal X-ray diffraction revealed that HIAM-210 crystallized in the monoclinic crystal system with a space group of *Pm* (Table S2†). The asymmetric unit of the structure contains ten independent Zn(II) centers coordinated in three fashions (Fig. S2†). Zn1, Zn3, Zn4, Zn7, Zn8, and Zn9 are tetrahedrally coordinated to two oxygen atoms from two NDC and two N atoms from two TZ ligands respectively; Zn2 and Zn6 are octahedrally bonded to two oxygen atoms from two NDC and four N atoms from four TZ ligands respectively; Zn5 and Zn10 are pentahedrally coordinated to three oxygen atoms from two NDC and two N atoms from two TZ ligands respectively. As depicted in Fig. 1b, each TZ ligand connects to three Zn(II) ions through $\mu_{1,2,4}$-bridging mode to form a 1D Zn–TZ chain along the *b*-axis, and the 1D chains are interconnected through NDC linkers to form a 2D Zn–TZ–NDC layer. The layers are further pillared by the linear ditopic carboxylate NDC by linking to two independent Zn(II) ions (Fig. 1c), constructing a 3D structure with 1D channels (Fig. 1d). It is noteworthy that this structure is different from the widely reported Zn–triazolate–dicarboxylate frameworks where the 2D layer was formed only by metal–triazolate coordination.[17–21] The compound features an unprecedented topology with point symbols $\{4^3\cdot5^2\cdot7\}\cdot\{4^3\cdot5^3\}_2\cdot\{4^3\}\cdot\{4^6\cdot5^2\cdot6^8\cdot7\cdot8^4\}\{4^6\cdot6^6\cdot8^3\}$ (Fig. S3†). The 1D channels of HIAM-210 were partitioned by benzene rings of NDC into arrays of interconnected cages with approximate sizes of 4.5 × 14.5 Å (Fig. 1e and S4†). As shown in Fig. 1f, multiple uncoordinated carboxylate–O atoms are unevenly distributed in four different cages, which have been believed to act as strong adsorption sites for hydrocarbons.[3,22,23]

The powder X-ray diffraction (PXRD) patterns of the as-synthesized and activated sample of HIAM-210 matched well with the simulated pattern, confirming its phase purity and structural integrity upon activation (Fig. S5†). N_2 adsorption–desorption measurement at 77 K was carried out to evaluate the porosity of HIAM-210 (Fig. 2a). The Brunauer–Emmett–Teller (BET) surface area and pore volume were calculated to be 565.96 $m^2\ g^{-1}$ and 0.24 $cm^3\ g^{-1}$, respectively and the pore size was centered at 4.02 Å established by the Horvath–Kawazoe method (inset, Fig. 2a), which is close to the kinetic diameter of C_2 hydrocarbons. Thermogravimetric (TG) analysis of the as-synthesized and activated HIAM-210 revealed that the latter has a longer plateau from 353 to 453 K. A thermal stability test by treating the compound under high temperature indicated that HIAM-210 maintained its structural integrity upon heating at 423 K for 3 days (Fig. S7†). To further verify its chemical stability, PXRD patterns were collected on samples immersed in

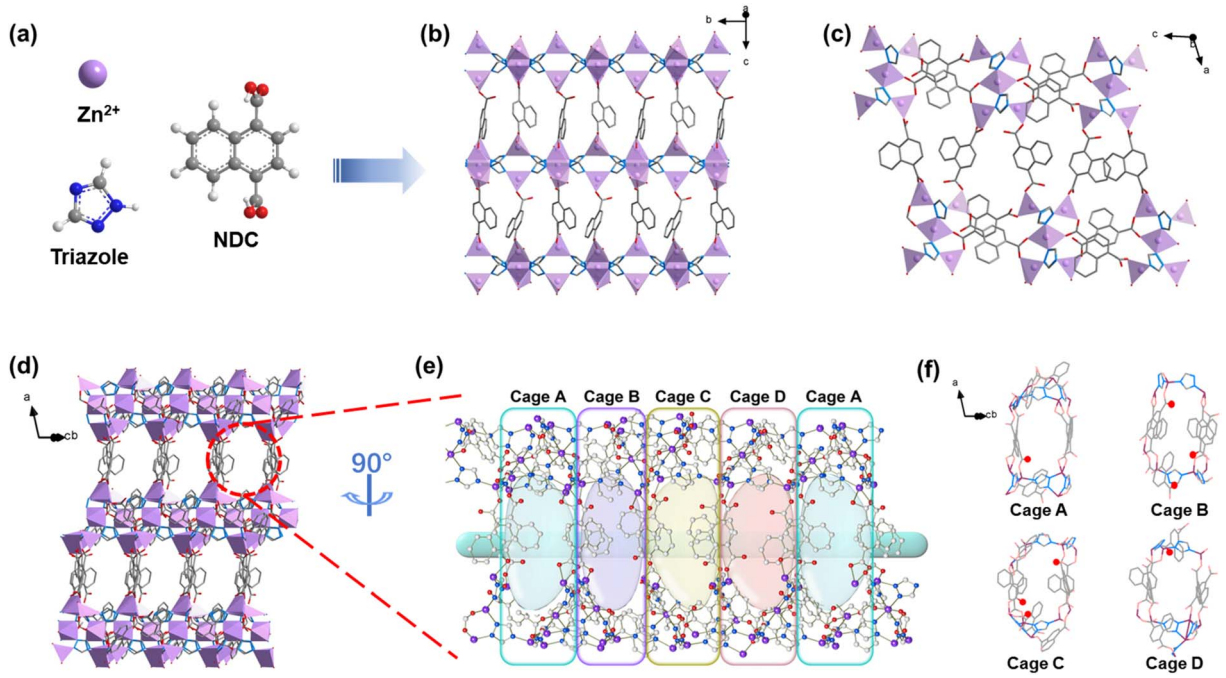

Fig. 1 Structure of HIAM-210. (a) The building blocks; (b) the 2D Zn–TZ–NDC layer structure; (c) the pillaring mode by NDC; (d) the structure viewed along the 1D channels; (e) a close-up view of the array of the four different cages in the channel; (f) the distribution of uncoordinated carboxylate–O atoms in the four cages.

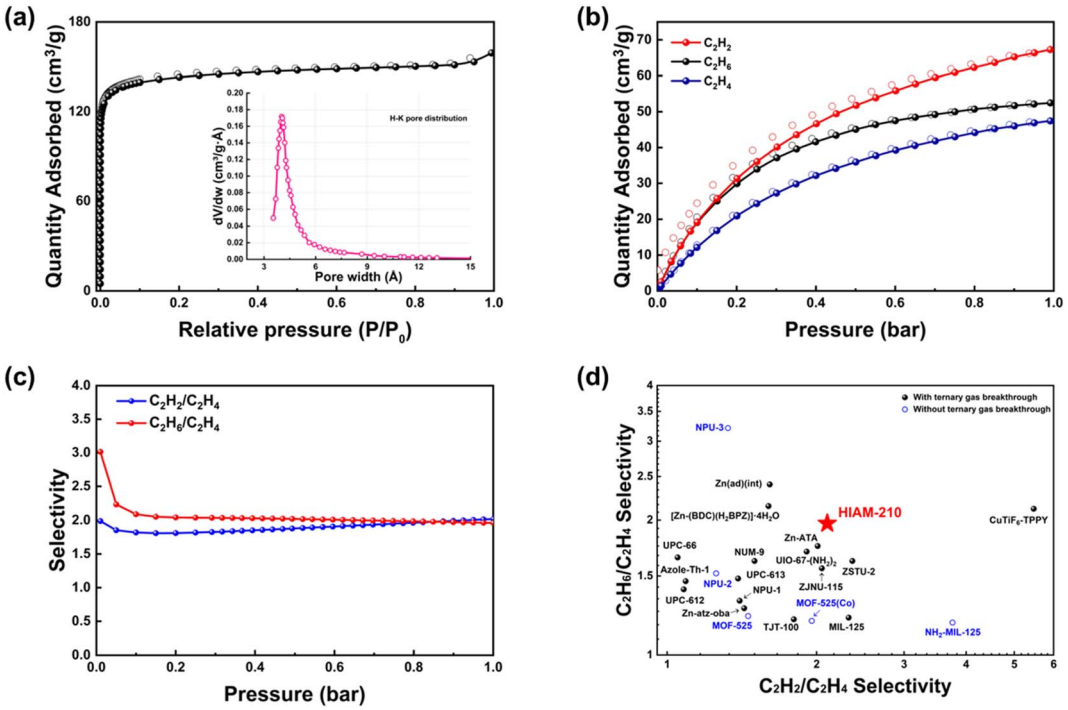

Fig. 2 Gas adsorption on HIAM-210. (a) N_2 adsorption–desorption isotherms at 77 K and pore size distribution (inset); (b) $C_2H_2/C_2H_4/C_2H_6$ adsorption–desorption isotherms at 298 K; (c) IAST selectivity of equimolar C_2H_2/C_2H_4 and C_2H_6/C_2H_4 mixtures at 298 K; (d) comparison of the separation performance of representative MOFs (C_2H_2/C_2H_4: 50/50, v/v; and C_2H_6/C_2H_4: 50/50, v/v).

water solutions with different pH values, and the results show that the structure of HIAM-210 remained intact under PH = 3 to 12 (Fig. S7†). The good stability, suitable pore size and delicate pore environment prompted us to further investigate the adsorption and separation ability of HIAM-210 for C_2 hydrocarbons.

Single-component adsorption isotherms of $C_2H_2/C_2H_4/C_2H_6$ for HIAM-210 were collected at 298 K and up to 1 bar, as shown in Fig. 2b. HIAM-210 adsorbs 52.44 $cm^3\ g^{-1}$ (7.04 wt%) of C_2H_6 and 67.26 $cm^3\ g^{-1}$ (7.82 wt%) of C_2H_2 at 1 bar and 298 K, higher than that of C_2H_4 (47.43 $cm^3\ g^{-1}$, 5.94 wt%) under identical conditions, showing preferential adsorption of C_2H_2 and C_2H_6 over C_2H_4. To access the separation capability for $C_2H_2/C_2H_4/C_2H_6$ mixtures, ideal adsorbed solution theory (IAST)[24] selectivities for the two binary mixtures (C_2H_2/C_2H_4 and C_2H_6/C_2H_4) were calculated and the dual-site Langmuir–Freundlich fitting parameters are shown in Table S3.† The calculated selectivities of C_2H_2/C_2H_4 and C_2H_6/C_2H_4 at 298 K and 1 bar are both 2.0, which are higher than those of most of the MOFs previously tested for $C_2H_2/C_2H_4/C_2H_6$ separation (Fig. 2d).[3,12–16,25–32] The isosteric heats of adsorption (Q_{st}) of C_2H_2, C_2H_4 and C_2H_6 on HIAM-210 were determined by using the Virial equation (Fig. S8 and S9†). The initial Q_{st} of C_2H_6 and C_2H_2 was 31.24 and 34.31 kJ mol^{-1}, respectively, higher than that of C_2H_4 (22.72 kJ mol^{-1}), suggesting that C_2H_6 and C_2H_2 have a relatively stronger interaction with the adsorbent than C_2H_4. It is worth noting that the Q_{st} curve of C_2H_2 shows a decrease followed by an increase with the gas loading. The decrease at low coverage is caused by the fact that adsorption sites with higher interaction energy are first occupied before the sites with lower energy. In contrast, the increase at higher coverage should be attributed to the attractive interactions between the adsorbed molecules.[33,34]

To reveal the preferential adsorption behavior of C_2H_6 and C_2H_2 over C_2H_4, GCMC simulation was carried out to study the preferential adsorption sites (see the ESI† for simulation detail). The simulation shows that the primary adsorption site is located at Cage C with two adjacent uncoordinated carboxylate–O atoms which can capture all three hydrocarbon molecules (Fig. 3a–c). The C_2H_2 molecule interacts strongly with the framework by forming multiple C–H···O hydrogen bonds with two uncoordinated O atoms (2.57 and 2.93 Å) and one coordinated O atom (2.70 Å). For C_2H_6, the adsorbed molecule forms multiple bonding interactions involving one C–H···π van der Waals (vdW) interaction (3.52 Å) with TZ, and three C–H···O hydrogen bonds with three O atoms (2.84–3.00 Å, including two uncoordinated and one coordinated one). In contrast, we found C_2H_4 is weakly adsorbed by longer bonding distances including three C–H···O hydrogen bonds with three O atoms (3.06–3.54 Å, including two uncoordinated and one coordinated one) and one C–H···π vdW interaction (3.43 Å) with TZ. The different interaction patterns between the gas and framework induced different binding energies with the trend of C_2H_2 (21.44 kJ mol^{-1}) > C_2H_6 (19.29 kJ mol^{-1}) > C_2H_4 (16.39 kJ mol^{-1}), obtained from DFT calculations. This trend is consistent with the sequences of adsorption isotherms and heats of adsorption. Moreover, we noticed a secondary adsorption site located in Cage B, which only adsorbs the C_2H_2 molecule (Fig. 3d). In Cage B, the C_2H_2 molecule also interacts with the uncoordinated

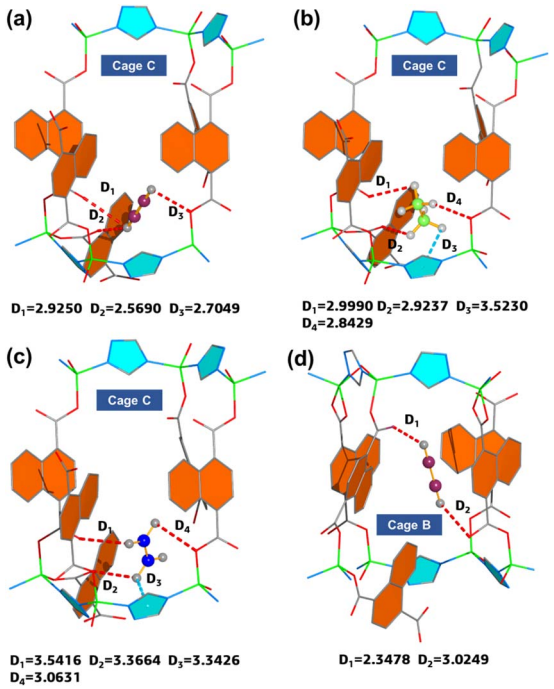

Fig. 3 The preferential adsorption sites for (a) C_2H_2, (b) C_2H_6, (c) C_2H_4 in Cage C and (d) preferential adsorption site for C_2H_2 in Cage B, and the C–H···π and C–H···O interactions are represented by blue and red dashed lines respectively.

carboxylate–O atoms to form short C–H···O hydrogen bonding interactions (2.35 and 3.02 Å). The above phenomenon indicates that the adjacent uncoordinated carboxylate–O atoms along the channels of HIAM-210 are crucial for the preferential recognition of C_2H_2 and C_2H_6 over C_2H_4.

To further evaluate the competitive adsorption of C_2H_2 and C_2H_6 on HIAM-210, GCMC simulation was conducted by introducing an equimolar binary mixture into the framework. The results show that C_2H_2 still occupies the primary binding sites within Cage C near the two adjacent uncoordinated carboxylate–O atoms. In contrast, C_2H_6 molecules tend to bind with uncoordinated carboxylate–O atoms in Cage A and Cage D (Fig. S10†). The results indicated that the binding energy of C_2H_2 in Cage C is higher than that of C_2H_6 at similar adsorption sites, which is consistent with the previous binding energy calculations.

Dynamic breakthrough experiments were further carried out to evaluate the feasibility of using HIAM-210 for the separation of C_2 binary and ternary mixtures. As depicted in Fig. 4a, b and S11,† HIAM-210 is capable of efficiently separating C_2H_4 from C_2H_2/C_2H_4 (50/50 and 1/99, v/v) and C_2H_6/C_2H_4 (50/50 and 10/90, v/v) binary mixtures. C_2H_4 always first eluted through the column to produce polymer-grade (>99.95%) C_2H_4. Breakthrough tests for ternary mixtures were subsequently performed. As shown in Fig. 4c, this compound can separate C_2H_4 from the equimolar ternary mixture. And breakthrough measurement with a gas mixture of $C_2H_2/C_2H_4/C_2H_6$ (1/90/9, v/v) that is close to the gas compositions in real applications was carried out. It was observed that C_2H_4 eluted out first at the 30th min, followed by C_2H_6 at the 38th min and C_2H_2 at the 39th min, producing polymer-grade C_2H_4 during the interval between the breakthrough of C_2H_4 and C_2H_6 with a productivity of 2.56 L kg^{-1} (Fig. 4d). Considering the potential interference and competitive adsorption of moisture in practical processes, we carried out a breakthrough experiment under a humid environment of 50% relative humidity (RH). As shown in Fig. 4e, the breakthrough curves and productivity of pure C_2H_4 under humid and dry environments were similar, demonstrating the

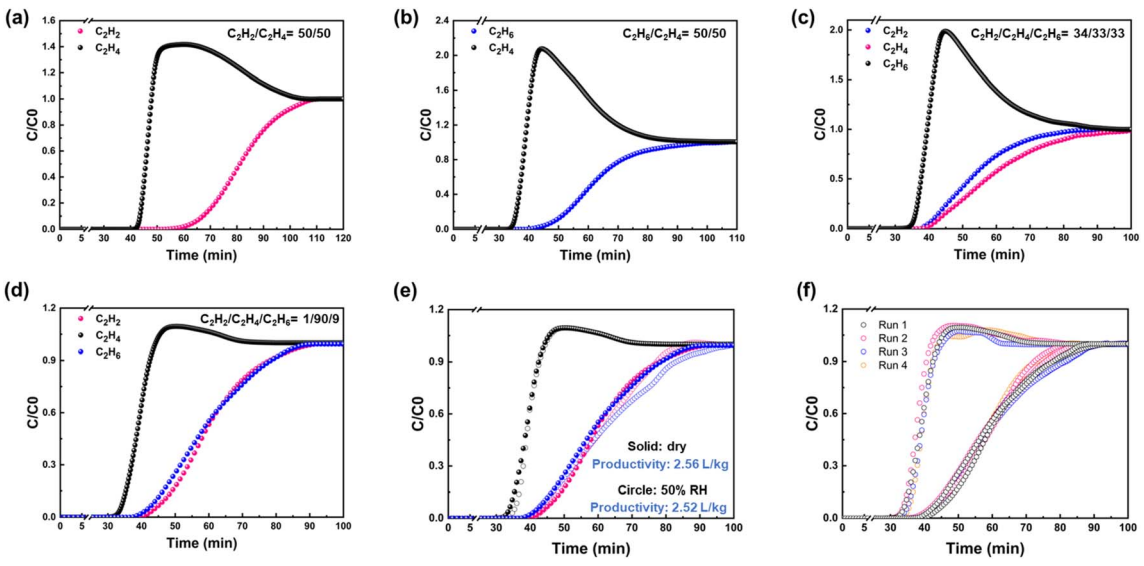

Fig. 4 Dynamic breakthrough tests on HIAM-210. The breakthrough curves for binary mixtures with the composition of (a) C_2H_2/C_2H_4 (50/50, v/v) and (b) C_2H_6/C_2H_4 (50/50, v/v), the breakthrough curves for ternary mixtures with the composition of (c) $C_2H_2/C_2H_4/C_2H_6$ (34/33/33, v/v/v) and (d) $C_2H_2/C_2H_4/C_2H_6$ (1/90/9, v/v/v), all collected at 298 K; (c) comparison of the breakthrough curves under humid and dry environments; (d) four consecutive breakthrough cycles at 298 K.

excellent water resistance of HIAM-210. To further evaluate the recyclability of the material, the adsorption column was regenerated under a helium flow (10 mL min^{-1}) at 373 K, and four consecutive breakthrough cycles were carried out. The results displayed no noticeable decrease of the separation capability of the adsorbent (Fig. 4f). The above tests suggest the durability of HIAM-210 for C_2H_4 purification under real-world industrial conditions.

Conclusions

In summary, we have developed a novel pillar-layer MOF (HIAM-210) combining a suitable pore size and optimal pore environment for simultaneous trapping of C_2H_2 and C_2H_6 from C_2H_2/C_2H_4/C_2H_6 ternary mixtures. HIAM-210 shows high selectivities for both C_2H_6/C_2H_4 and C_2H_2/C_2H_4. Dynamic breakthrough tests confirmed the outstanding separation performance of HIAM-210 for one-step purification of C_2H_4 from C_2H_2/C_2H_4/C_2H_6 ternary mixtures, with high recyclability and strong resistance to moisture. GCMC calculations and DFT calculations demonstrated that the uncoordinated carboxylate–O atoms were the origin of the preferential adsorption. This work not only provides a promising candidate for C_2H_4 purification but also offers insights into tailoring the pore environments of MOFs for highly efficient gas separations.

Data availability

The data that support the findings of this study are available in the ESI† of this article.

Author contributions

H. Wang and J. Li designed the project. J. Liu synthesized the compounds, conducted and analyzed the PXRD, adsorption, and breakthrough tests. J. Liu, H. Wang, and J. Li wrote the first draft and all authors contributed to the discussion of the final draft.

Conflicts of interest

There are no conflicts to declare.

Acknowledgements

This work is financially supported by the Shenzhen Science and Technology Program (No. JCYJ20190809145615620, RCYX20200714114539243, and KCXFZ20211020163818026), Post-doctoral Foundation Project of Shenzhen Polytechnic (6022330001K) and China Postdoctoral Science Foundation (2022M713278).

Notes and references

1 P. Q. Liao, W. X. Zhang, J. P. Zhang and X. M. Chen, Efficient purification of ethene by an ethane-trapping metal-organic framework, *Nat. Commun.*, 2015, **6**, 8697.

2 L. Li, R. B. Lin, R. Krishna, H. Li, S. Xiang, H. Wu, J. Li, W. Zhou and B. Chen, Ethane/ethylene separation in a metal-organic framework with iron-peroxo sites, *Science*, 2018, **362**, 443–446.

3 Q. Ding, Z. Zhang, Y. Liu, K. Chai, R. Krishna and S. Zhang, One-Step Ethylene Purification from Ternary Mixtures in a Metal-Organic Framework with Customized Pore Chemistry and Shape, *Angew. Chem., Int. Ed. Engl.*, 2022, **61**, e202208134.

4 Y. Yoshimura, N. Kijima, T. Hayakawa, K. Murata, K. Suzuki, F. Mizukami, K. Matano, T. Konishi, T. Oikawa and M. Saito, Catalytic cracking of naphtha to light olefins, *Catal. Surv. Jpn.*, 2001, **4**, 157–167.

5 K.-J. Chen, D. G. Madden, S. Mukherjee, T. Pham, K. A. Forrest, A. Kumar, B. Space, J. Kong, Q.-Y. Zhang and M. J. Zaworotko, Synergistic sorbent separation for one-step ethylene purification from a four-component mixture, *Science*, 2019, **366**, 241–246.

6 W. Zheng, Y. Wang, B. Wang, M. Fan, L. Ling and R. Zhang, C_2H_2 Selective Hydrogenation to C_2H_4: Engineering the Surface Structure of Pd-Based Alloy Catalysts to Adjust the Catalytic Performance, *J. Phys. Chem. C*, 2021, **125**, 15251–15261.

7 P. Zhang, L. Yang, X. Liu, J. Wang, X. Suo, L. Chen, X. Cui and H. Xing, Ultramicroporous material based parallel and extended paraffin nano-trap for benchmark olefin purification, *Nat. Commun.*, 2022, **13**, 4928.

8 X. Cui, K. Chen, H. Xing, Q. Yang, R. Krishna, Z. Bao, H. Wu, W. Zhou, X. Dong and Y. Han, Pore chemistry and size control in hybrid porous materials for acetylene capture from ethylene, *Science*, 2016, **353**, 141–144.

9 P. A. Webley, Adsorption technology for CO_2 separation and capture: a perspective, *Adsorption*, 2014, **20**, 225–231.

10 M. Eddaoudi, J. Kim, N. Rosi, D. Vodak, J. Wachter, M. O'Keeffe and O. M. Yaghi, Systematic design of pore size and functionality in isoreticular MOFs and their application in methane storage, *Science*, 2002, **295**, 469–472.

11 H. Deng, S. Grunder, K. E. Cordova, C. Valente, H. Furukawa, M. Hmadeh, F. Gandara, A. C. Whalley, Z. Liu, S. Asahina, H. Kazumori, M. O'Keeffe, O. Terasaki, J. F. Stoddart and O. M. Yaghi, Large-pore apertures in a series of metal-organic frameworks, *Science*, 2012, **336**, 1018–1023.

12 H. G. Hao, Y. F. Zhao, D. M. Chen, J. M. Yu, K. Tan, S. Ma, Y. Chabal, Z. M. Zhang, J. M. Dou, Z. H. Xiao, G. Day, H. C. Zhou and T. B. Lu, Simultaneous Trapping of C_2H_2 and C_2H_6 from a Ternary Mixture of C_2H_2/C_2H_4/C_2H_6 in a Robust Metal-Organic Framework for the Purification of C_2H_4, *Angew. Chem., Int. Ed. Engl.*, 2018, **57**, 16067–16071.

13 L. Fan, P. Zhou, X. Wang, L. Yue, L. Li and Y. He, Rational Construction and Performance Regulation of an In(III)-Tetraisophthalate Framework for One-Step Adsorption-Phase Purification of C(2)H(4) from C(2) Hydrocarbons, *Inorg. Chem.*, 2021, **60**, 10819–10829.

14 S. Q. Yang, F. Z. Sun, P. Liu, L. Li, R. Krishna, Y. H. Zhang, Q. Li, L. Zhou and T. L. Hu, Efficient Purification of Ethylene from C_2 Hydrocarbons with an C_2H_6/C_2H_2-

Selective Metal-Organic Framework, *ACS Appl. Mater. Interfaces*, 2021, **13**, 962–969.

15 B. Zhu, J. W. Cao, S. Mukherjee, T. Pham, T. Zhang, T. Wang, X. Jiang, K. A. Forrest, M. J. Zaworotko and K. J. Chen, Pore Engineering for One-Step Ethylene Purification from a Three-Component Hydrocarbon Mixture, *J. Am. Chem. Soc.*, 2021, **143**, 1485–1492.

16 Y. Wang, M. Fu, S. Zhou, H. Liu, X. Wang, W. Fan, Z. Liu, Z. Wang, D. Li, H. Hao, X. Lu, S. Hu and D. Sun, Guest-molecule-induced self-adaptive pore engineering facilitates purification of ethylene from ternary mixture, *Chem*, 2022, **8**, 3263–3274.

17 K.-J. Chen, R.-B. Lin, P.-Q. Liao, C.-T. He, J.-B. Lin, W. Xue, Y.-B. Zhang, J.-P. Zhang and X.-M. Chen, New Zn-Aminotriazolate-Dicarboxylate Frameworks: Synthesis, Structures, and Adsorption Properties, *Cryst. Growth Des.*, 2013, **13**, 2118–2123.

18 N. Bai, S. n. Li, Y. Jiang, M. Hu and Q. Zhai, Pillar-layered Zn–triazolate–carboxylate frameworks tuned by the bend angles of ditopic ligands, *Inorg. Chem. Commun.*, 2015, **53**, 84–87.

19 F. ZareKarizi, M. Joharian and A. Morsali, Pillar-layered MOFs: functionality, interpenetration, flexibility and applications, *J. Mater. Chem. A*, 2018, **6**, 19288–19329.

20 X.-L. Yan, S.-N. Li, Y.-C. Jiang, M.-C. Hu and Q.-G. Zhai, Synthesis, crystal structures and gas adsorption of two porous pillar-layered MOFs decorated with different functional groups, *Inorg. Chem. Commun.*, 2015, **62**, 107–110.

21 Y. Ling, Z. X. Chen, F. P. Zhai, Y. M. Zhou, L. H. Weng and D. Y. Zhao, A zinc(II) metal-organic framework based on triazole and dicarboxylate ligands for selective adsorption of hexane isomers, *Chem. Commun.*, 2011, **47**, 7197–7199.

22 L. Yang, L. Yan, Y. Wang, Z. Liu, J. He, Q. Fu, D. Liu, X. Gu, P. Dai, L. Li and X. Zhao, Adsorption Site Selective Occupation Strategy within a Metal-Organic Framework for Highly Efficient Sieving Acetylene from Carbon Dioxide, *Angew. Chem., Int. Ed. Engl.*, 2021, **60**, 4570–4574.

23 Y.-Z. Li, G.-D. Wang, W.-J. Shi, L. Hou, Y.-Y. Wang and Z. Zhu, Efficient C_2H_n Hydrocarbons and VOC Adsorption and Separation in an MOF with Lewis Basic and Acidic Decorated Active Sites, *ACS Appl. Mater. Interfaces*, 2020, **12**, 41785–41793.

24 A. L. Myers and J. M. Prausnitz, Thermodynamics of mixed-gas adsorption, *AIChE J.*, 1965, **11**, 121–127.

25 Q. Ding, Z. Zhang, P. Zhang, C. Yu, C.-H. He, X. Cui and H. Xing, One-step ethylene purification from ternary mixture by synergetic molecular shape and size matching in a honeycomb-like ultramicroporous material, *Chem. Eng. J.*, 2022, **450**, 138272.

26 Z. Xu, X. Xiong, J. Xiong, R. Krishna, L. Li, Y. Fan, F. Luo and B. Chen, A robust Th-azole framework for highly efficient purification of C_2H_4 from a $C_2H_4/C_2H_2/C_2H_6$ mixture, *Nat. Commun.*, 2020, **11**, 3163.

27 G. D. Wang, Y. Z. Li, W. J. Shi, L. Hou, Y. Y. Wang and Z. Zhu, One-Step C_2H_4 Purification from Ternary $C_2H_6/C_2H_4/C_2H_2$ Mixtures by a Robust Metal-Organic Framework with Customized Pore Environment, *Angew. Chem., Int. Ed. Engl.*, 2022, e202205427, DOI: **10.1002/anie.202205427**.

28 Y. Wang, C. Hao, W. Fan, M. Fu, X. Wang, Z. Wang, L. Zhu, Y. Li, X. Lu, F. Dai, Z. Kang, R. Wang, W. Guo, S. Hu and D. Sun, One-step Ethylene Purification from an Acetylene/Ethylene/Ethane Ternary Mixture by Cyclopentadiene Cobalt-Functionalized Metal-Organic Frameworks, *Angew. Chem., Int. Ed. Engl.*, 2021, **60**, 11350–11358.

29 X. W. Gu, J. X. Wang, E. Wu, H. Wu, W. Zhou, G. Qian, B. Chen and B. Li, Immobilization of Lewis Basic Sites into a Stable Ethane-Selective MOF Enabling One-Step Separation of Ethylene from a Ternary Mixture, *J. Am. Chem. Soc.*, 2022, **144**, 2614–2623.

30 P. Liu, Y. Wang, Y. Chen, J. Yang, X. Wang, L. Li and J. Li, Construction of saturated coordination titanium-based metal–organic framework for one-step $C_2H_2/C_2H_6/C_2H_4$ separation, *Sep. Purif. Technol.*, 2021, **276**, 119284.

31 P. Zhang, Y. Zhong, Y. Zhang, Z. Zhu, Y. Liu, Y. Su, J. Chen, S. Chen, Z. Zeng and H. Xing, Synergistic binding sites in a hybrid ultramicroporous material for one-step ethylene purification from ternary C_2 hydrocarbon mixtures, *Sci. Adv.*, 2022, **8**, eabn9231.

32 J. W. Cao, S. Mukherjee, T. Pham, Y. Wang, T. Wang, T. Zhang, X. Jiang, H. J. Tang, K. A. Forrest, B. Space, M. J. Zaworotko and K. J. Chen, One-step ethylene production from a four-component gas mixture by a single physisorbent, *Nat. Commun.*, 2021, **12**, 6507.

33 S. Hlushak, Heat of adsorption, adsorption stress, and optimal storage of methane in slit and cylindrical carbon pores predicted by classical density functional theory, *Phys. Chem. Chem. Phys.*, 2018, **20**, 872–888.

34 S. Sen, S. Neogi, A. Aijaz, Q. Xu and P. K. Bharadwaj, Construction of non-interpenetrated charged metal-organic frameworks with doubly pillared layers: pore modification and selective gas adsorption, *Inorg. Chem.*, 2014, **53**, 7591–7598.